Int. J. Heat Mass Transfer. Vol. 15, pp. 1467–1475. Pergamon Press 1972. Printed in Great Britain

ON STEADY LAMINAR FREE CONVECTION DUE TO A HEATED ELLIPSOID OF REVOLUTION

A. WATSON and G. POOTS

Department of Applied Mathematics, The University of Hull, Hull, Yorkshire, England

(*Received* 29 *April* 1971 *and in revised form* 25 *October* 1971)

Abstract—Numerical solutions are presented for the three-dimensional free convection boundary layer due to a heated ellipsoid of revolution. Flow and heat-transfer characteristics are given in graphical form.

NOMENCLATURE

$\boldsymbol{a}_1$, $\boldsymbol{a}_2$,	unit vectors on the surface;
a, b,	minor and major axis of ellipsoid;
c_p,	specific heat;
Gr,	Grashof number;
h_1, h_2,	length elements;
$\boldsymbol{i}$, $\boldsymbol{j}$, $\boldsymbol{k}$,	Cartesian unit vectors;
k,	thermal conductivity of the fluid;
$\boldsymbol{n}$,	unit normal to the surface;
Nu,	Nusselt number:
Pr,	Prandtl number;
$\boldsymbol{r} = \boldsymbol{r}(x_1, x_2)$,	position vector of a point on the surface;
t,	time;
T,	temperature;
$\boldsymbol{v}$,	velocity vector in the boundary layer;
V_J/θ_J	velocity and thermal field functions;
x, y, z,	Cartesian coordinates;
x_1, x_2, x_3,	coordinates.

Greek symbols

α,	a/b, reciprocal of the aspect ratio;
β,	coefficient of cubical expansion;
μ,	viscosity;
ν,	kinematic viscosity;
τ_1, τ_2,	shear stress components;
ρ,	density;
θ,	dimensionless temperature.

Subscripts

∞,	ambient condition;
w,	wall condition.

1. INTRODUCTION

TO DATE there is a lack of theoretical information on three-dimensional free convection flows. Although the governing flow equations are readily formulated their numerical solution is difficult owing to their nonlinear nature and the availability of computer storage.

It is the purpose of this paper to present some quantitative information on the three-dimensional free convection boundary layer due to a heated ellipsoid of revolution. The boundary layer equations employed to describe this 'boundary-sheet' flow have already been formulated for incompressible forced flow by Watson [1] and later extended to include the effect of a buoyancy force by Poots [2]. The latter employed such equations to investigate laminar free convection near the lower stagnation point on an isothermal general curved surface.

2. THE BOUNDARY LAYER EQUATIONS

Following [1] and [2], and employing intrinsic orthogonal coordinates x_1 and x_2

on the surface with x_3 measured along the normal to the surface. the velocity field may be represented by

$$\boldsymbol{v} = v_1\boldsymbol{a}_1 + v_2\boldsymbol{a}_2 + v_3\boldsymbol{n}. \tag{1}$$

where $\boldsymbol{n} = \boldsymbol{a}_1 \times \boldsymbol{a}_2$ and $\boldsymbol{a}_1$ and $\boldsymbol{a}_2$ are unit vectors tangential to the parametric lines for x_2 and x_1 constant. respectively. If T denotes the temperature then the boundary layer equations. given in the notation of [1] and [2]. are:

$$\frac{1}{h_1h_2}\left\{\frac{\partial}{\partial x_1}(h_2v_1) + \frac{\partial}{\partial x_2}(h_1v_2)\right\} + \frac{\partial v_3}{\partial x_3} = 0. \tag{2}$$

$$\rho\left(\frac{\mathrm{D}v_1}{\mathrm{D}t} + \frac{v_1v_2}{h_1h_2}\frac{\partial h_1}{\partial x_2} - \frac{v_2^2}{h_1h_2}\frac{\partial h_2}{\partial x_1}\right) = (\rho - \rho_\infty)g\boldsymbol{n}_0 \cdot \boldsymbol{a}_1 + \mu\frac{\partial^2 v_1}{\partial x_3^2}. \tag{3}$$

$$\rho\left(\frac{\mathrm{D}v_2}{\mathrm{D}t} + \frac{v_1v_2}{h_1h_2}\frac{\partial h_2}{\partial x_1} - \frac{v_1^2}{h_1h_2}\frac{\partial h_1}{\partial x_2}\right) = (\rho - \rho_\infty)g\boldsymbol{n}_0 \cdot \boldsymbol{a}_2 + \mu\frac{\partial^2 v_2}{\partial x_3^2}. \tag{4}$$

and

$$\rho c_p\frac{\mathrm{D}T}{\mathrm{D}t} = k\frac{\partial^2 T}{\partial x_3^2}. \tag{5}$$

where

$$\frac{\mathrm{D}}{\mathrm{D}t} = \frac{v_1}{h_1}\frac{\partial}{\partial x_1} + \frac{v_2}{h_2}\frac{\partial}{\partial x_2} + v_3\frac{\partial}{\partial x_3}.$$

and the unit vector $\boldsymbol{n}_0$ is in the downward vertical direction. The equation of state is

$$\rho - \rho_\infty = -\rho_\infty\beta(T - T_\infty). \tag{6}$$

where the suffix ∞ is used to denote the condition at T_∞. the ambient temperature.

The boundary conditions for an isothermal surface are:

$$\left.\begin{aligned} &\boldsymbol{v} = 0. \quad T = T_w \text{ on } x_3 = 0 \text{ for all } x_1.\ x_2. \\ &v_1 \to 0. \quad v_2 \to 0. \quad T - T_\infty. \text{ as } x_3 \to \infty \text{ for all } x_1\ x_2. \end{aligned}\right\} \tag{7}$$

and it is assumed that $T_w > T_\infty$.

3. ANALYSIS FOR AN ELLIPSOID OF REVOLUTION

Consider a heated ellipsoid of revolution defined by

$$\frac{x^2}{a^2} + \frac{y^2}{a^2} + \frac{z^2}{b^2} = 1. \tag{8}$$

whose axis of revolution is horizontal; the lower stagnation point is located at $(0.\ -a.\ 0)$. Orthogonal parametric coordinates are chosen so that the surface is given vectorially by

$$\boldsymbol{r} = a\cos x_1\sin x_2\boldsymbol{i} - a\cos x_1\cos x_2\boldsymbol{j} - b\sin x_1\boldsymbol{k}. \tag{9}$$

where $\boldsymbol{i}.\ \boldsymbol{j}$ and $\boldsymbol{k}$ denote unit Cartesian vectors. The lower stagnation point is at $x_1 = x_2 = x_3 = 0$ and $\boldsymbol{n}_0 = -\boldsymbol{j}$ (see Fig. 4A). Standard formulae. see Weatherburn [3]. yield:

$$\left.\begin{aligned} h_1 &= (a^2\sin^2 x_1 + b^2\cos^2 x_1)^{\frac{1}{2}}. \qquad h_2 = a\cos x_1. \\ \boldsymbol{n}_0 \cdot \boldsymbol{a}_1 &= -a\sin x_1\cos x_2/h_1. \\ \boldsymbol{n}_0 \cdot \boldsymbol{a}_2 &= -\sin x_2. \end{aligned}\right\} \tag{10}$$

For convenience introduce the dimensionless variables.

$$\left.\begin{aligned} &X_1 = x_1. \quad X_2 = x_2. \qquad X_3 = Gr^{\frac{1}{4}}x_3/a. \\ &V_1 = \frac{a}{\nu}Gr^{-\frac{1}{2}}v_1. \quad V_2 = \frac{a}{\nu}Gr^{-\frac{1}{2}}v_2. \\ &V_3 = \frac{a}{\nu}Gr^{-\frac{1}{4}}v_3. \end{aligned}\right\} \tag{11}$$

and

$$\theta = (T - T_\infty)/(T_w - T_\infty).$$

together with the dimensionless length elements

$$H_j = h_j/a \text{ for } j = 1.\ 2.$$

Substitution of (10) and (11) into the governing equations (2)–(5) yields the following dimensionless system of equations:

$$\frac{\partial}{\partial x_1}(H_1V_2) + H_1\frac{\partial v_2}{\partial x_2} + H_1H_2\frac{\partial v_3}{\partial x_3} = 0. \tag{12}$$

$$\mathscr{L}(V_1) - \frac{V_2^2}{H_1 H_2}\frac{\partial H_2}{\partial X_1} = \frac{\partial^2 V_1}{\partial X_3^2} + \frac{1}{H}\theta \sin X_1 \cos X_2. \quad (13)$$

$$\mathscr{L}(V_2) + \frac{V_1 V_2}{H_1 H_2}\frac{\partial H_2}{\partial X_1} = \frac{\partial^2 V_2}{\partial X_3^2} + \theta \sin X_2. \quad (14)$$

$$Pr\, \mathscr{L}(\theta) = \frac{\partial^2 \theta}{\partial V_3^2}. \quad (15)$$

where

$$\mathscr{L} = \frac{V_1}{H_1}\frac{\partial}{\partial X_1} + \frac{V_2}{H_2}\frac{\partial}{\partial X_2} + V_3\frac{\partial}{\partial X_3}$$

and $Pr = c_p\mu/k$ is the Prandtl number. The boundary conditions (7) become

$$\left.\begin{aligned} &V = 0.\quad \theta = 1 \quad \text{on } X_3 = 0 \\ &\qquad\qquad \text{for all } X_1, X_2. \\ &\text{and} \\ &V_1 \to 0.\quad V_2 \to 0.\ \theta \to 0 \text{ as } X_3 \to \infty \\ &\qquad\qquad \text{for all } X_1, X_2. \end{aligned}\right\} \quad (16)$$

Clearly a full numerical solution of the above system of nonlinear parabolic type differential equations would require excessive amounts of computing time and storage. However, preliminary quantitative results are obtained on seeking expansion of the form;

$$\left.\begin{aligned} &V_1 = X_1(V_1 + X_1^2 V_{11} + 0(X_1^4)). \\ &V_2 = X_2(V_{20} + X_1^2 V_{21} + 0(X_1^4)). \\ &V_3 = V_{30} + X_1^2 V_{31} + 0(X_1^4). \\ &\text{and} \\ &\theta = \theta_0 + X_1^2\theta_1 + 0(X_1^4). \end{aligned}\right\} \quad (17)$$

where the functions V_{ij} and θ_j depend on X_2 and X_3. There are two reasons for favouring expansions of the form (17). Firstly it is expedient to do so since the length elements (10) are functions of X_1 only. Secondly as the aspect ratio b/a tends to infinity the limiting configuration is a horizontal circular cylinder and the velocity and thermal fields become two-dimensional and so independent of the variable X_1.

Substitution of (17) into the governing equations (12)–(16) yields the following:

Zeroth order equations for $V_{10}, V_{20}, V_{30}, \theta_0$

$$\alpha V_{10} + \frac{\partial}{\partial X_2}(X_2 V_{20}) + \frac{\partial V_{30}}{\partial X_3} = 0. \quad (18)$$

$$X_2 V_{20}\frac{\partial V_{10}}{\partial X_2} + V_{30}\frac{\partial V_{10}}{\partial X_3} + \alpha(V_{10}^2 + X_2^2 V_{20}^2) = \frac{\partial^2 V_{10}}{\partial X_3^2} + \alpha\theta_0 \cos X_2. \quad (19)$$

$$V_{20}\frac{\partial}{\partial X_2}(X_2 V_{20}) + V_{30}\frac{\partial V_{20}}{\partial X_3} = \frac{\partial^2 V_{20}}{\partial X_3^2} + \frac{\sin X_2}{X_2}\theta_0. \quad (20)$$

and

$$Pr\left(X_2 V_{20}\frac{\partial \theta_0}{\partial X_2} + V_{30}\frac{\partial \theta_0}{\partial X_3}\right) = \frac{\partial^2 \theta_0}{\partial X_3^2}. \quad (21)$$

The boundary conditions are:

$$\left.\begin{aligned} &V_{10} = V_{20} = V_{30} = 0.\quad \theta_0 = 1 \\ &\qquad\qquad \text{for } X_3 = 0.\quad \text{all } X_2. \\ &V_{10} \to 0.\quad V_{20} \to 0.\quad \theta \to 0 \\ &\qquad\qquad \text{as } X_3 \to \infty.\quad \text{all } X_2. \end{aligned}\right\} \quad (22)$$

First order equations for $V_{11}, V_{21}, V_{31}, \theta_1$

$$3\alpha V_{11} - \frac{\alpha}{2}(1+\alpha^2)V_{10} + \frac{\partial}{\partial X_2}(X_2 V_{21}) + \frac{1}{2}\frac{\partial}{\partial X_2}(X_2 V_{10}) + \frac{\partial V_{31}}{\partial X_3} = 0. \quad (23)$$

$$X_2 V_{20}\frac{\partial V_{11}}{\partial X_2} + X_2\left(V_{21} + \frac{1}{2}V_{20}\right)\frac{\partial V_{10}}{\partial X_2} + V_{30}\frac{\partial V_{11}}{\partial X_3} + V_{31}\frac{\partial V_{10}}{\partial X_3} + \alpha\left\{4V_{10}V_{11} + 2X_2^2 V_{20}V_{21} + \frac{1}{2}(1-\alpha^2)V_{10}^2 + \tfrac{1}{6}(5-3\alpha^2)X_2^2 V_{20}^2\right\} = \frac{\partial^2 V_{11}}{\partial X_3^2} + \alpha\{\theta_1 + \tfrac{1}{6}(2-3\alpha^2)\theta_0\}\cos X_2. \quad (24)$$

$$V_{20}\frac{\partial}{\partial X_2}(X_2V_{21}) + \left(V_{21} + \frac{1}{2}V_{20}\right)\frac{\partial}{\partial X_2}(X_2V_{20}) + V_{30}\frac{\partial V_{21}}{\partial X_3} + V_{31}\frac{\partial V_{20}}{\partial X_3} + \alpha V_{10}(2V_{21} - V_{20}) = \frac{\partial^2 V_{21}}{\partial X_3^2} + \theta_1\frac{\sin X_2}{X_2}. \quad (25)$$

and

$$Pr\left\{X_2V_{20}\frac{\partial\theta_1}{\partial X_2} + X_2\left(V_{21} + \frac{1}{2}V_{20}\right)\frac{\partial\theta_0}{\partial X_2} + V_{30}\frac{\partial\theta_1}{\partial X_3} + V_{31}\frac{\partial\theta_0}{\partial X_3} + 2\alpha V_{10}\theta_1\right\} = \frac{\partial^2\theta_1}{\partial X_3^2}. \quad (26)$$

The boundary conditions are:

$$\left.\begin{aligned} &V_{11} = V_{21} = V_{31} = \theta_1 = 0 \text{ for } X_3 = 0. \text{ all } X_2. \\ &V_{11} \to 0,\ V_{21} \to 0,\ \theta_1 \to 0 \quad \text{as } X_3 \to \infty. \quad \text{all } X_2. \end{aligned}\right\} \quad (27)$$

4. NUMERICAL SOLUTIONS

Numerical solutions of the nonlinear equations (18)–(22) and the linear equations (23)–(27) have been obtained for air, taking $Pr = 0{\cdot}72$ and $\alpha = 0.\ \frac{1}{8}.\ \frac{1}{4}.\ \frac{1}{2}$ and 1; note that the limiting values $\alpha = 0$ and 1 correspond to free convection flows for a heated circular cylinder and sphere respectively.

The step-by-step integration along the surface in the X_2-direction was accomplished by employing the Hartree–Womersley method [4]. Along the normal to the surface in the X_3-direction, a matrix interpretative scheme based on quasi-linearization was utilized.

It was found necessary in the vicinity of the stagnation point to employ a step length $\Delta X_3 = 0{\cdot}1$, for the range $0 \leqslant X_3 \leqslant 8$, so as to obtain close agreement with the stagnation point solutions given in [2]. For the region $0 \leqslant X_2 \leqslant \pi/2$ the boundary layer is adequately contained within the range $0 \leqslant X_3 \leqslant 8$ and to maintain accuracy a step length $\Delta X_2 = 0{\cdot}1$ was necessary. Now in the limiting case of the cylinder it is known from experimental observation, when Gr is large, that a convection plume is initiated at $X_2 = 2{\cdot}7$. approximately (see Howarth [5]). Moreover. in the vicinity of the plume the first order boundary layer approximation used to formulate (2)–(5) is invalid. Consequently integrations have been terminated at $X_2 = 2{\cdot}5$. To cope with the thickening of the boundary layer in the region $\pi/2 \leqslant X_2 \leqslant 2{\cdot}5$ the range of integration in the X_3-direction was increased to 12 units with $\Delta X_3 = 0{\cdot}1$ as before.

With regard to the truncation of the series expansions (17) the solutions so obtained will be valid only for a limited region of the surface. In order to establish the domain of validity of these expansions the case of the sphere. $\alpha = 1$. was considered in some detail. This case. whilst being the simplest to investigate geometrically. is worst from the viewpoint of convergence of the expansions in the variable X_1. Thus the azimuthal velocity component

$$v_\phi = (V_1 \sin X_2 - V_2 \sin X_1 \text{ as } X_2) / (1 - \cos^2 X_1 \cos^2 X_2)^{\frac{1}{2}}, \quad (28)$$

when evaluated from (17). is not zero for all X_1. Stipulating that the magnitude of v_ϕ should be less than one per cent. say. of the maximum velocity throughout the boundary layer provides a possible criterion for the determination of the limiting values of X_2 given X_1. For $X_1 = 0{\cdot}4$ and $0{\cdot}8$ the estimated limits on X_2 were $X_2 = 2{\cdot}4$ $2{\cdot}0$. respectively. An independent check on this domain of validity may be made by comparing values of the meridional velocity component.

$$v_m = (V_1 \sin X_1 \text{ as } X_2 + V_2 \sin X_2) / (1 - \cos^2 X_1 \cos^2 X_2)^{\frac{1}{2}}, \quad (29)$$

at stations where $\cos X_1 \cos X_2 = \text{const.}$ i.e. along lines of latitude. It was found that. within the above limiting values on X_1 and X_2. the change in v_m was less than one per cent of its value at $X_1 = 0$ for any given line of latitude.

In the following section flow and heat transfer results are presented graphically for various α. In this discussion the above limiting values on X_1 and X_2 are adhered to in all cases. Note that

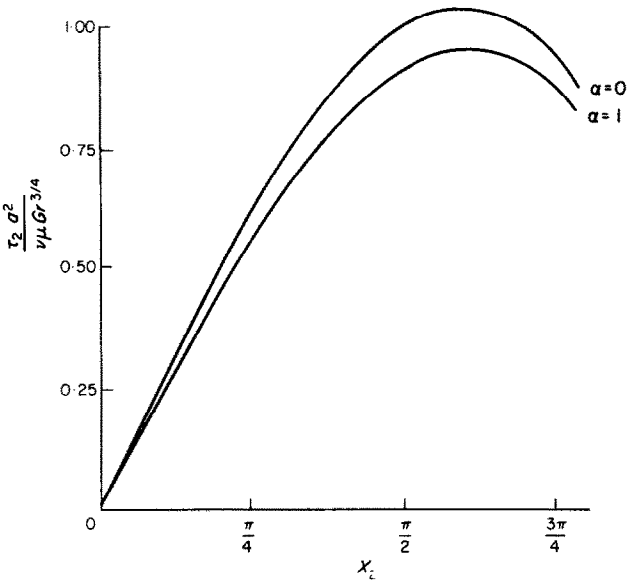

FIG. 1. The dimensionless shear stress $\tau_2 a^2/(\nu\mu Gr^{\frac{3}{4}})$ for various α, $X_1 = 0{\cdot}0$.

in the special case $\alpha = 0$ the solutions are independent of the X_1-coordinate. However, when $X_1 \neq 0$ certain limiting values of the results are given by curves marked $\alpha \to 0$. Such curves form a bound at fixed X_1, for the results as α decreases. However they are not, in general, the same as those obtained by putting $\alpha = 0$ in the governing equations.

5. DISCUSSION OF RESULTS

Shear stress components

These are defined by

$$\tau_1 = \mu \left(\frac{\partial v_1}{\partial x_3}\right)_w \text{ and } \tau_2 = \mu \left(\frac{\partial v_2}{\partial x_3}\right)_w \tag{30}$$

Dimensionless shear stress components $\tau_j a^2/(\nu\mu Gr^{\frac{3}{4}})$ are displayed in Figs. 1–3 for various α at stations $X_1 = 0{\cdot}0$ and $0{\cdot}8$.

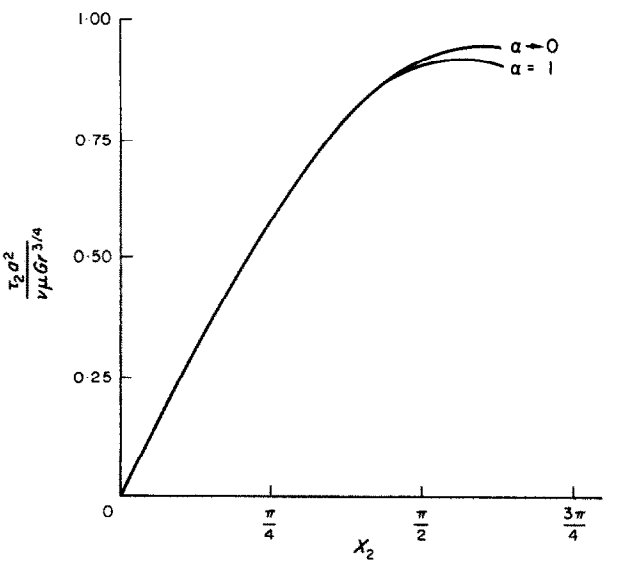

FIG. 2. The dimensionless shear stress $\tau_2 a^2/(\nu\mu Gr^{\frac{3}{4}})$ for various α, $X_1 = 0{\cdot}8$.

Consider first the component $\tau_2(0.\ X_2;\ \alpha)$ given in Fig. 1. Clearly variations with α are of order 5 per cent. In the special case of a horizontal cylinder the shear stress increases from zero at the lower stagnation point and attains a maximum slightly beyond $X_2 = \pi/2$. From then onwards it decreases rapidly so as to

Limiting streamlines

The equations for the limiting streamlines are

$$x_3 = 0. \quad \frac{h_1 dx_1}{\tau_1} = \frac{h_2 dx_2}{\tau_2}. \tag{31}$$

To enhance the pictorial description of the limiting streamlines isometric elevations of half

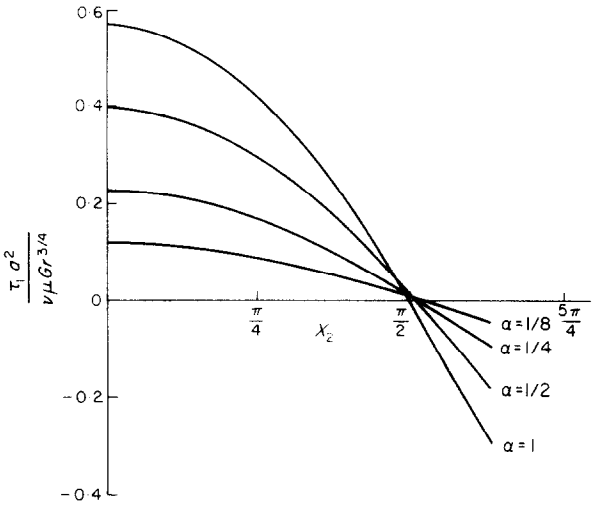

FIG. 3. The dimensionless shear stress $\tau_1 a^2/(\nu\mu G r^{\frac{1}{4}})$ for various α. $X_1 = 0{\cdot}8$.

adjust itself to conditions in the vicinity of the plume. This trend occurs as a result of a maximum in the buoyancy force at $X_2 = \pi/2$; the momentum generated in the accelerated region produces the observed maximum after $X_2 = \pi/2$. Moreover, the effects of local curvature (α varying) are greatest for small X_1. Hence at station $X_1 = 0{\cdot}8$ the component $\tau_2(0{\cdot}8.\ X_2;\ \alpha)$ is seen in Fig. 2 to be virtually independent of α in the accelerated region.

Owing to symmetry $\tau_1(0.\ X_2;\ \alpha)$ is identically zero. For non-zero X_1 the component τ_1 will increase with increasing α. Since the flow in the upper half of the ellipsoid adjusts itself to the plume condition, a reversal in the sign of τ_1 would be expected near $X_2 = \pi/2$. These features are clearly seen in Fig. 3.

of the ellipsoid are presented in Figs. 4(a) and 5(a) for $\alpha = \frac{1}{4}$ and $\frac{1}{2}$, respectively; in Figs. 4(b) and 5(b) are the corresponding plan views of the limiting streamlines emerging from the lower stagnation point. In both views the streamlines were constructed in the $(X_1,\ X_2)$-plane and then transformed into the appropriate physical coordinates for each plot (see Watson [6]). The figures are self-explanatory. For example in the case of $\alpha = \frac{1}{4}$, see Figs. 5(a) and 5(b), the flow in the line of symmetry $X_1 = 0$ is virtually two-dimensional; curvature effects in the X_1-direction distort the streamlines as displayed and are more pronounced for X_1 near to $\pi/2$.

Heat transfer

The local wall heat transfer is given in terms

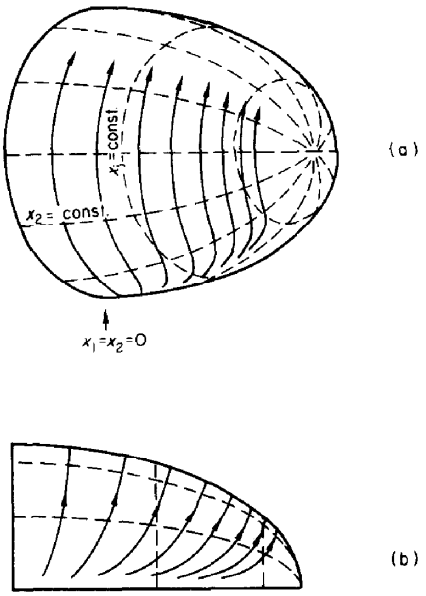

FIG. 4(a). Limiting streamlines in isometric elevation for $\alpha = \frac{1}{2}$.

FIG. 4(b). Limiting streamlines in plan view of the lower stagnation point for $\alpha = \frac{1}{2}$.

of the dimensionless Nusselt number

$$Nu = -\left(\frac{\partial\theta}{\partial X_3}\right)_{X_3=0} Gr^{\frac{1}{4}}. \tag{32}$$

Consider the variation of $Nu/Gr^{\frac{1}{4}}$ on the line of symmetry $X_1 = 0$, see Fig. 6. For any α the heat transfer is greatest at the lower stagnation point and decreases slowly in the accelerated region and much more rapidly thereafter; these effects are more pronounced with increasing α. Similar trends occur for $X_1 = 0{\cdot}8$ as seen from Fig. 7. Note that the effects of local curvature on heat transfer, as with τ_2, are more important near the line of symmetry $X_1 = 0$.

CONCLUSIONS

Preliminary numerical results have been given for the steady free convection boundary layer due to a heated ellipsoid of revolution. Because of the method of series expansion information is limited and cannot be provided, for example, on the behaviour of the limiting streamlines in the vicinity of the plume region. However the

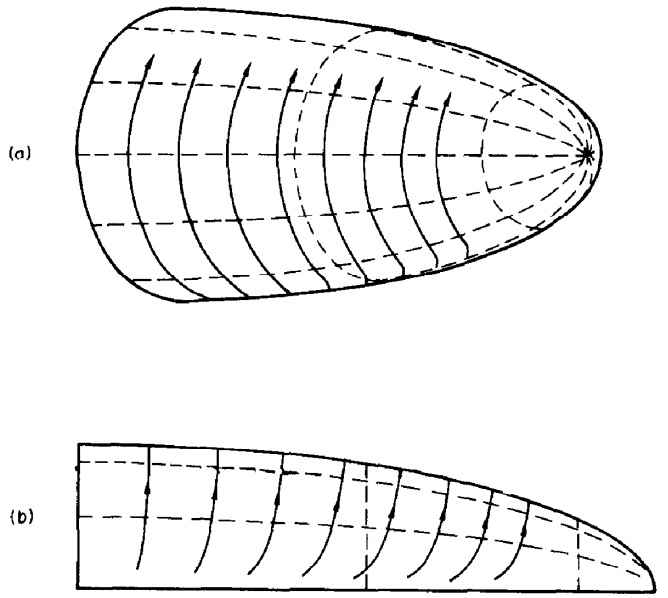

FIG. 5(a). Limiting streamlines in isometric elevation for $\alpha = \frac{1}{4}$.
FIG. 5(b). Limiting streamlines in plan view of the lower stagnation point for $\alpha = \frac{1}{4}$.

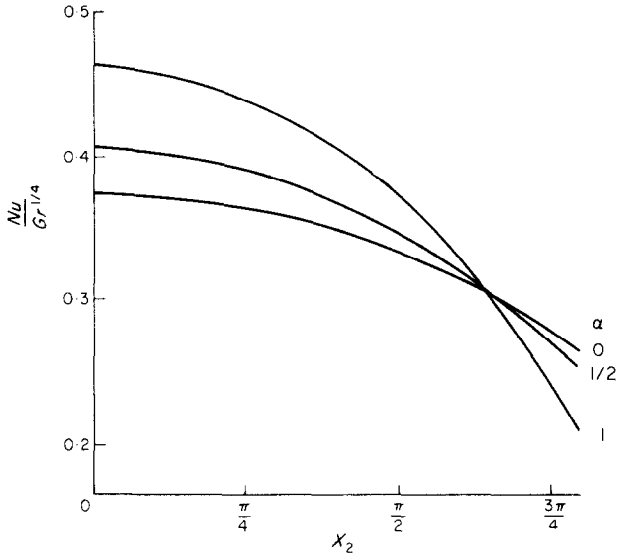

FIG. 6. Nusselt number for $X_1 = 0{\cdot}0$ for various α.

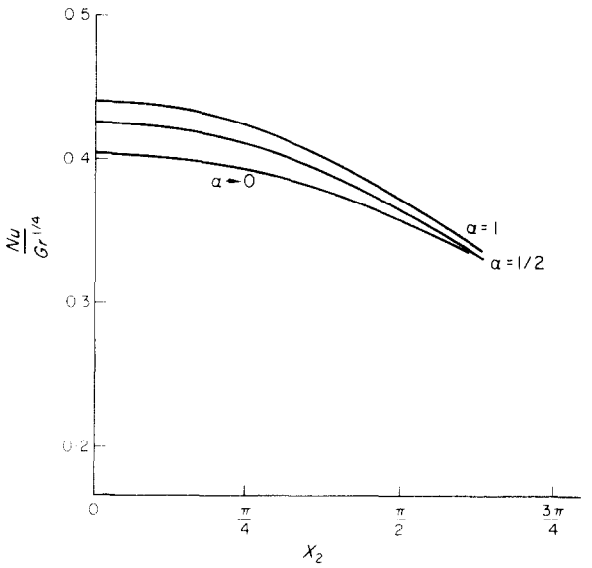

FIG. 7. Nusselt number for $X_1 = 0{\cdot}8$ for various α.

material presented should prove valuable as a test of accuracy in a full scale numerical study of the problem.

REFERENCES

1. E. J. WATSON. *Laminar Boundary Layers*, edited by L. ROSENHEAD. University Press, Oxford (1963).
2. G. POOTS, Laminar free convection near the lower stagnation point on an isothermal curved surface, *Int. J. Heat Mass Transfer* **7**, 863–874 (1964).
3. C. E. WEATHERBURN, *Differential Geometry of Three Dimensions*. Vol. 1. University Press, Cambridge (1927).
4. D. R. HARTREE, A solution of the laminar boundary layer equations, *Proc. R. Soc.* **164A**, 547–579 (1933).
5. L. HOWARTH (editor), *Modern Developments in Fluid Dynamics, High Speed Flow*. Vol. 2, p. 813. Clarendon Press, Oxford (1964).
6. A. WATSON, Numerical studies of two and three dimensional convection flows, Ph.D. Thesis, University of Hull (1971).

SUR LA CONVECTION NATURELLE LAMINAIRE ET PERMANENTE DUE À UN ELLIPSOÏDE DE RÉVOLUTION CHAUFFÉ.

Résumé—On présente des solutions numériques pour la couche limite tridimensionnelle de convection naturelle autour d'un ellipsoïde de révolution chauffé. Les aspects caractéristiques de l'écoulement et du transfert thermique sont donnés sous forme graphique.

STATIONÄRE LAMINARE FREIE KONVEKTION AN EINEM BEHEIZTEN ROTATIONSELLIPSOID

Zusammenfassung—Für die dreidimensionale freie Konvektionsgrenzschicht an einem beheizten Rotationsellipsoid werden numerische Lösungen angegeben.

Charakteristika der Strömung und des Wärmeübergangs sind grafisch wiedergegeben.

О СТАЦИОНАРНОЙ ЛАМИНАРНОЙ СВОБОДНОЙ КОНВЕКЦИИ ОТ НАГРЕТОГО ЭЛЛИПСОИДА ВРАЩЕНИЯ

Аннотация—Представлены численные решения для трехмерного пограничного слоя при свободной конвекции на нагретом эллипсоиде вращения. Графически представлены характеристики течения и теплообмена.